Mon. Not. R. Astron. Soc. **324,** 1102–1108 (2001)

Discovery of molecular hydrogen line emission associated with methanol maser emission

J.-K. Lee,★† A. J. Walsh,‡ M. G. Burton and M. C. B. Ashley
School of Physics, University of New South Wales, Sydney, NSW 2052, Australia

Accepted 2001 February 6. Received 2001 February 6; in original form 2000 March 9

ABSTRACT

We report the discovery of H_2 line emission associated with 6.67-GHz methanol maser emission in massive star-forming regions. In our UNSWIRF/AAT observations, H_2 1–0 S(1) line emission was found associated with an ultracompact H II region IRAS 14567–5846 and isolated methanol maser sites in G318.95–0.20, IRAS 15278–5620 and IRAS 16076–5134. Owing to the lack of radio continuum in the latter three sources, we argue that their H_2 emission is shock excited, while it is UV-fluorescently excited in IRAS 14567–5846. Within the positional uncertainties of 3 arcsec, the maser sites correspond to the location of infrared sources. We suggest that 6.67-GHz methanol maser emission is associated with hot molecular cores, and propose an evolutionary sequence of events for the process of massive star formation.

Key words: masers – stars: formation – ISM: lines and bands – ISM: molecules – infrared: ISM.

1 INTRODUCTION

6.7 GHz methanol (CH_3OH) maser emission in the $5_1–6_0A^+$ transition is one of the strongest astrophysical masers. Since the first detection by Menten (1991), it has been established as a tracer of massive star-forming regions, often containing ultracompact (UC) H II regions (e.g. Caswell et al. 1995; Slysh et al. 1999). However it is not clear how the masers are related to the physical process of massive star formation, and how they are associated with UC H II regions. Norris et al. (1993, 1998) and Phillips et al. (1998) proposed that the methanol maser emission comes from circumstellar discs. Menten (1996) suggested that it comes from warm shells around UC H II regions, and Walsh et al. (1998) suggested that the maser emission occurs behind shocks.

Walsh et al. (1997, 1998; hereafter Papers I and II, respectively) investigated the association between methanol masers and UC H II regions by carrying out low and high spatial resolution radio surveys. They found that methanol maser emission usually occurs in massive star-forming regions, but only 25 per cent (46 out of 232) of maser sites were found close to an UC H II region, contrary to expectations. To explain this, they hypothesized an evolutionary sequence, where methanol maser emission commences during an early phase of pre-main-sequence evolution of massive stars, before being destroyed as the star creates an UC H II region.

★E-mail: jkl@cp.dias.ie
† Present address: Dublin Institute of Advanced Studies, 5 Merrion Sq., Dublin 2, Ireland.
‡ Present address: Max-Planck-Institut für Radioastronomie, auf dem Hügel 69, Bonn D-53121, Germany.

This hypothesis can be tested by searching for other indicators of star formation, such as deeply embedded infrared (IR) or sub-millimetre sources and outflows, associated with the maser emission. Walsh et al. (1999; hereafter Paper III) carried out a near-IR (NIR) survey to identify embedded stellar counterparts to the UC H II regions and maser sources. Using the positional coincidences and colours of the NIR sources, they identified about half (12 out of 25) of the maser sites and about two-thirds (12 out of 18) of UC H II regions with a NIR counterpart, i.e. proportionately more maser sites are found to have no observable NIR counterpart than UC H II regions. From this, they concluded that maser sites are associated with more deeply embedded objects than UC H II regions are.

In an attempt to extend this work, we have searched for H_2 1–0 S(1) line emission in the NIR, as a tracer of outflow activity associated with the early stages of star formation. Here we report the discovery of H_2 line emission associated with methanol maser sites. This is the first part of a larger survey for H_2 emission associated with either the UC H II regions and/or the methanol masers.

2 OBSERVATIONS AND DATA REDUCTION

The sources listed in Table 1 were observed in H_2 1–0 S(1) 2.12-μm line emission using the University of New South Wales Infrared Fabry–Perot (UNSWIRF; Ryder et al. 1998) on the 3.9-m Anglo-Australian Telescope (AAT). The UNSWIRF is a narrow-band ($\lambda/\delta\lambda \sim 4000$) tunable filter for the NIR, used in conjunction with the 128 × 128 pixel Infrared Imager and Spectrometer (IRIS;

Allen et al. 1993). Used at *f*/36, it produces a circular image of 100 arcsec diameter with a pixel scale of 0.8 arcsec. The velocity resolution is 75 km s^{-1} full width at half-maximum (FWHM). The observations were made on 1997 July 23 and 1998 June 16.

Table 1. List of sources observed by the UNSWIRF/AAT. The source names are given in the first column, with their position in the second and third columns. The range of V_{lsr} for the methanol maser emission is presented in the fourth column, and these values are from Paper II.

Source Name	Coordinates R.A. (J2000)	Dec. (J2000)	V_{lsr} (km s^{-1})
	UC H II region		
IRAS 14567−5846	15 00 35.0	−58 58 10	–
	Methanol Maser Sites		
G318.95−0.20	15 00 55.4	−58 58 53	−38.2 to −32.0
IRAS 15278−5620	15 31 45.4	−56 30 50	−47.7 to −56.3; −57.4
IRAS 16076−5134	16 11 26.6	−51 41 57	−85.2 to −78.3

The observing sequence with UNSWIRF included one off-line setting (for continuum subtraction) and several on-line Fabry–Perot (FP) spacings, equally spaced at 39 km s^{-1} about the line centre, determined by the maser radial velocities. This sequence was carried out with a few minutes integration time for each FP spacing, first on a source and then on a sky position, for both sky and continuum subtraction. An integration time of 3 min was used for IRAS 14567–5846 and G318.95−0.20 and 2 min for IRAS 15278−5620 and 16076−5134. A standard star was imaged at each of the FP settings for flux calibration, as was a diffuse dome lamp to obtain a flat field.

For data reduction, bias subtraction and linearization were performed during readout using a non-destructive readout method. The object frames were sky-subtracted, and then flat-fielded by normalized dome flat-fields at matching FP settings. All frames are then registered using field stars in the continuum frame. For continuum subtraction, the continuum frame is scaled based on the photometric result of a standard star and subtracted from all other on-line frames. The line flux and central velocities of the H_2 emission were then determined through Lorentzian fitting of

Table 2. Results from the UNSWIRF observation of H_2 1–0 S(1) line emission. The source name is given in the first column, followed by the observed velocity range of H_2 emission in the second. The peak and integrated flux of H_2 line emission are given in the third and fourth columns, respectively. The distance to the sources and the luminosity of H_2 1–0 S(1) line emission are in the fifth and sixth columns.

Source name	ΔV_{H_2} (km s^{-1})	$F_{peak}(H_2)$ ($\times 10^{-16}$ erg s^{-1} cm^{-2} arcsec^{-2})	$F_{int}(H_2)$ ($\times 10^{-13}$ erg s^{-1} cm^{-2})	Distance (kpc)	L[H_2 1–0 S(1)] ($\times 10^{-1}$ $L_\odot$)
		UC H II region			
IRAS 14567−5846	∼20	3 ± 6%	0.7	2.4	0.1
		Methanol Maser Sites			
G318.95−0.20	≥50	17* ± 2%	≥1*	2.4	≥0.2
IRAS 15278−5620	∼70	17 ± 2%	10	3.6	4.0
IRAS 16076−5134	∼15	8 ± 3%	2	5.6	1.6

* A lower limit for F_{peak} and F_{int}, with insufficient FP coverage of the H_2 emission.

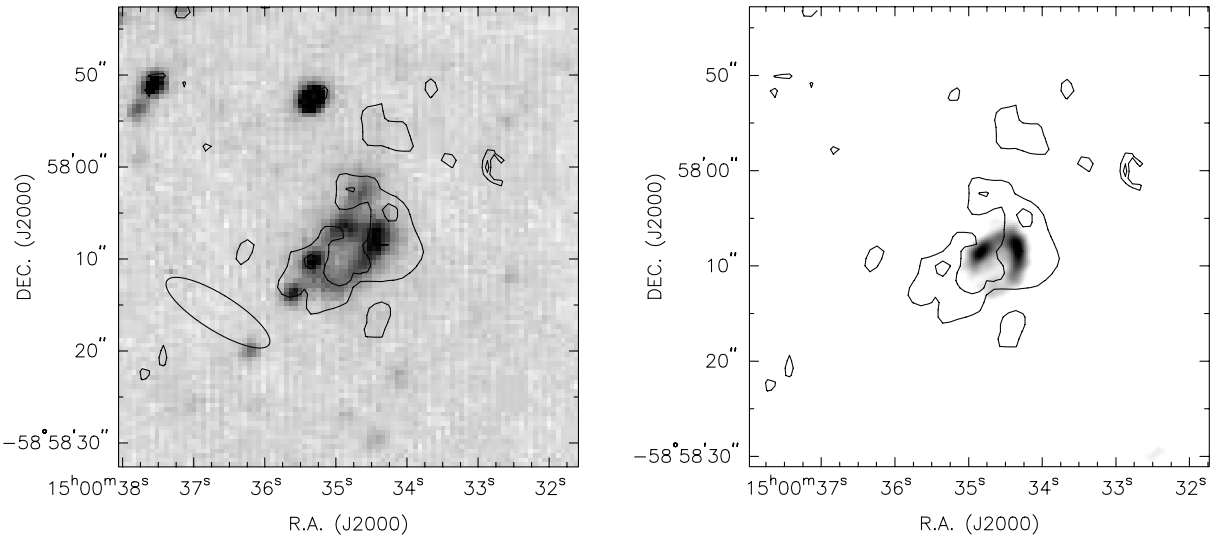

Figure 1. Left: the UNSWIRF image of the IRAS 14567–5846 UC H II region. The H_2 1–0 S(1) 2.12-μm line emission is drawn in contours, and a 2.2-μm continuum image as a grey-scale (Paper III). Contour levels are 1.3 and 2.3 × 10^{-16} erg cm^{-2} s^{-1} arcsec^{-2}. The ellipse indicates the IRAS error ellipse. Right: the H_2 line emission map (contours) overlaid on the 6.67-GHz radio continuum image (grey-scale) from Paper I. The same contour levels are used. H_2 emission encompasses the 2.2-μm continuum nebulosity as well as the radio continuum (Paper II).

on-line frames stacked into a cube of increasing etalon spacing, or wavelength. The absolute flux measurement involves ∼30 per cent error, and the absolute velocity can be measured, based on comparison with that of known H_2-emitting sources, to within 15 to 20 km s^{-1} accuracy. Meanwhile, relative velocity differences between emitting regions in a source can be discerned when they are ≥10 km s^{-1}. The data were reduced mostly with a customized program using IRAF routines. A detailed UNSWIRF data reduction procedure can be found in Ryder et al. (1998).

3 RESULTS

Results from our UNSWIRF observation of H_2 line emission associated with one UC H II region and three methanol maser sites are summarized in Table 2. Features for individual sources are described below. The source names are from Paper II, with other common names also provided in square brackets. The images of 2.2-μm broad-band *K*-band continuum emission are displayed in comaprison with H_2 line emission. They are from Paper III as they have superior quality to those of our narrow-band continuum obtained by UNSWIRF.

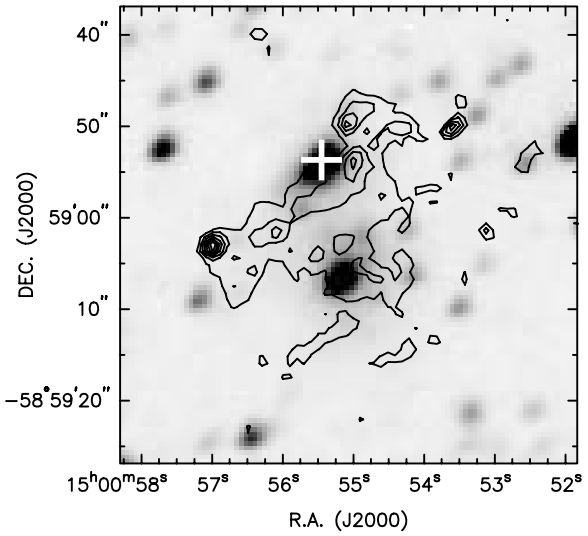

Figure 2. The UNSWIRF image of maser site G318.95–0.20, with grey-scale (2.2-μm continuum) and contours (H_2 line) as in Fig. 1. This source is located 2.5 arcmin to the SE of Fig. 1. The plus sign marks the position of the methanol maser site from Paper II. Contours are from 2, 4, 6, 8, 10, 12 and 14×10^{-16} erg cm^{-2} s^{-1} arcsec^{-2}.

3.1 IRAS 14567−5846

A large bright cometary UC H II region is associated with this IRAS source (Paper II). No methanol maser emission is found associated with this source. The extent of the UC H II region is approximated by the 2.2-μm *K*-band continuum emission, seen in grey-scale at the centre of Fig. 1. Weak H_2 emission, represented by the contours, appears to surround the UC H II region in a shell. The observed velocity structure has line centre velocities varying within a 20 km s^{-1} range. We do not expect to see any velocity structure with our spectral resolution as other UC H II regions show expansion velocities of typically 5 km s^{-1} (Kawamura & Masson 1998).

3.2 G318.95−0.20

This maser site is located about 2.5 arcmin to the south-east (SE) of the cometary UC H II region discussed above. The range of maser radial velocities is $V_{\rm lsr} = -38.2$ to -32.0 km s^{-1}. No radio continuum emission is found associated with this maser site above the 5σ detection limit of 0.8 mJy (Ellingsen, Norris & McCulloch 1996). The H_2 emission here is much stronger than that associated with the UC H II region above (Fig. 2). The emission feature extends over 30 arcsec (∼0.4 pc at the distance of 2.4 kpc) from the maser site, and outflow morphology is not clear in the intensity map. Our FP spacings turned out to be insufficient to cover all the emission, making unreliable the estimate of the H_2 line flux and central velocities. The velocity map is not presented; however, we

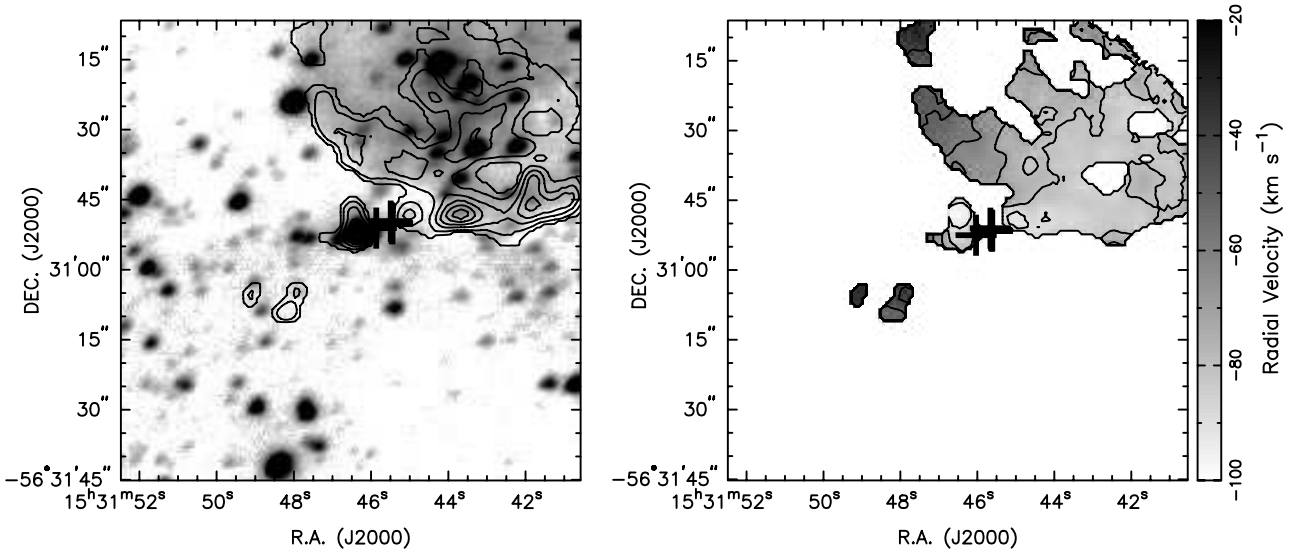

Figure 3. Left: the UNSWIRF image of IRAS 15278–5620, with the grey-scale (2.2-μm continuum) and contour (H_2 line) maps as in Fig. 1. The plus signs indicate the positions of methanol maser sites. Contour levels are 2.5, 5.0, 7.5, 10.0, 12.5 and 15.0×10^{-16} erg cm^{-2} s^{-1} arcsec^{-2}. Extended H_2 emission is seen to the N and NW, close to and to the SE of the masersites. Right: the line centre velocity map of H_2 emission in both grey-scale and contours. Contour levels are −90, −80, −70, −60, −50 and −40 km s^{-1}.

note from a Lorentzian fitting of the available frames that the velocity of the H_2 emission extends over at least 50 km s^{-1}.

3.3 IRAS 15278−5620 [G323.74−0.26]

Two methanol maser sites ($V_{lsr} = -47.7$ to -56.3 and -57.4 km s^{-1}; separated by 5 arcsec) were found associated with two embedded NIR sources (Paper III). The maser sites are located to the SE of a cluster of stars which exhibit 2.2-μm continuum nebulosity. The UNSWIRF observation reveals fan-shaped H_2 emission north-west (NW) of the maser sites with weak emission to the SE (Fig. 3). The 2.2-μm continuum emission extends over a larger area than the H_2 line emission does.

The velocity maps (Figs 3 and 4) show three components with the line centre velocities smoothly changing about a 70 km s^{-1} range (-93 to -25 km s^{-1}). Two redshifted components are seen; one being weak redshifted emission to the SE, and the other ∼30 arcsec N of the maser sites. The third component is blueshifted emission to the NW of the maser sites. The second red component appears to be connected to the blueshifted component.

3.4 IRAS 16076−5134 [G331.28−0.19]

A knot, slightly elongated along the R.A. axis, is seen 10 arcsec to the west of the maser site in the 2.2-μm continuum image (Paper III), pointing towards, but stopping short of, the maser site ($V_{lsr} = -85.2$ to -78.3 km s^{-1}; Fig. 5). Our UNSWIRF data show it is H_2 emission, and the H_2 line centre velocities range over 13 km s^{-1} (-55 to -68 km s^{-1}), redshifted relative to the maser emission velocity. Weaker H_2 emission is also present to the south-west (SW) of the maser site, with velocity ranging from -63 to -44 km s^{-1}.

4 DISCUSSION

All sources show excited H_2 line emission at 2.12-μm, and the H_2 emission associated with the UC H II region is weaker than that associated with the methanol maser sites. In this section we discuss

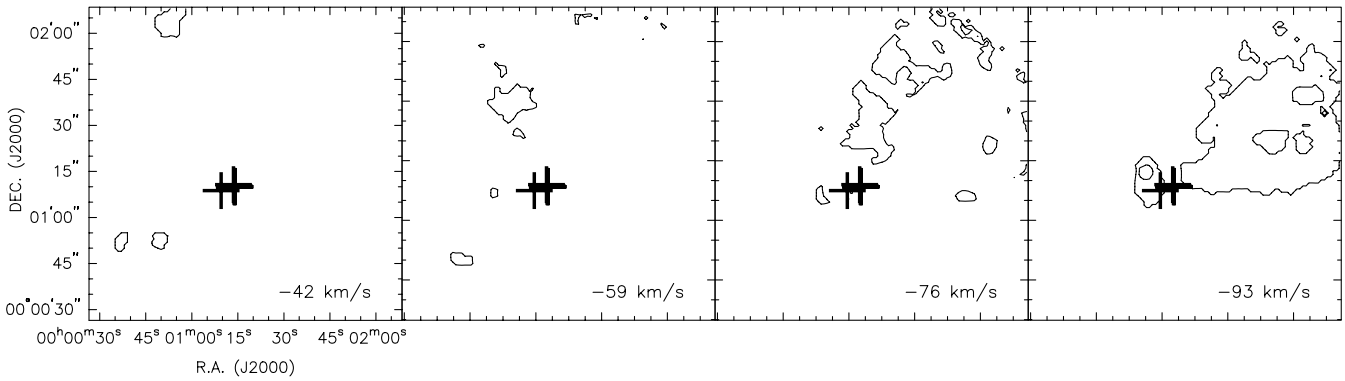

Figure 4. Maps of the H_2 line emission centre velocity for IRAS 15278−5620. The plus signs again mark the position of methanol maser sites. From left to right, each panel shows velocity components at $-42, -59, -76$ and -93 km s^{-1}. The redshifted components in the first and second panels are clearly separated from the blueshifted components in the fourth.

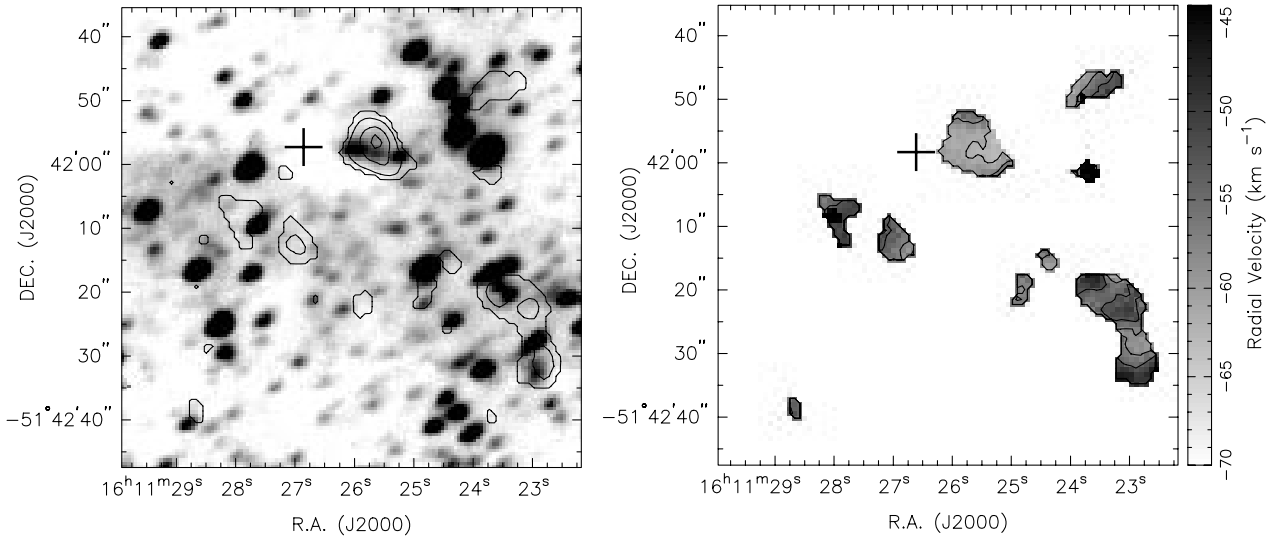

Figure 5. Left: the UNSWIRF image of IRAS 16076–5134, both in grey-scale (continuum) and contours (H_2 line) as in Fig. 1. Contour levels are 2, 4, 6 and 8×10^{-16} erg cm^{-2} s^{-1} arcsec^{-2}. The H_2 emission peaks to the west of a masersite, and coincides with a *K*-band feature elongated in the R.A. direction. Right: the line centre velocity map as in Fig. 3. Contour levels are -65, -60 and -55 km s^{-1}.

the excitation mechanism of the H_2, the implications for the origin of the methanol maser emission, and its role in the sequence of events that produce massive stars.

4.1 Excitation of H_2 – shocked or fluorescent?

H_2 emission in the 1–0 S(1) line is usually attributed to either radiative excitation by UV photons (e.g. Burton 1992) or collisional excitation in shocks (Hollenbach & McKee 1989). The intensity ratio of the 1–0 S(1) line to the 2–1 S(1) line is a diagnostic often used to distinguish the excitation mechanism. With no 2–1 S(1) line intensity available, we refer instead to morphology and line velocities to infer the origin of the H_2 emission.

UV fluorescence seems likely for IRAS 14567–5846, where the H_2 emission appears to surround the UC H II region, forming a photodissociation region (PDR) around an ionized bubble. In all other cases, no radio continuum emission (from ionized gas which requires UV photons) was reported in Paper II. Thus this absence of UV photons associated with methanol maser sites suggests that shock excitation of H_2 is the most likely mechanism. For G318.95−0.02 the morphology does not allow us to distinguish between shocks and fluorescence, however the broad linewidth ($>50\,\mathrm{km\,s^{-1}}$) suggests it is shock-excited.

IRAS 15278–5620 is a complex case with three velocity components, as described in Section 3. The wide radial velocity range and the morphology of the blueshifted lobe to the NW and the redshifted lobe to the SE are suggestive of outflow, thus shock excitation of the H_2 emission. The possibility that the H_2 emission comes from a rotating disc is excluded because the mass required for an arcmin-long structure rotating at about $40\,\mathrm{km\,s^{-1}}$ is of order $10^5\,M_\odot$. Although the NW blueshifted component overlaps somewhat with a redshifted component to the N in Fig. 3, the large difference in radial velocities between the two (Fig. 4) suggests a different origin.

IRAS 16076–5134 shows strong H_2 emission about 10 arcsec west of methanol maser sites with blueshifted line velocities from the maser radial velocity. Weak redshifted H_2 emission is also present, approximately on the opposite side of the maser site. Such line velocities and morphology are also suggestive of outflow, therefore shock excitation of the H_2 emission seems likely. A mid-IR source is reported coincident with the maser site at 10.5 μm by Walsh et al. (2001), while it did not show up at 3.3 μm (Paper III). This must therefore be a highly embedded object, and possibly powers the outflow.

4.2 Origin of methanol maser emission

There has been debate as to where, in relation to sites of star formation, methanol maser emission occurs. Two plausible hypotheses put forward are that it arises (1) within circumstellar discs (Norris et al. 1993) and (2) associated with shocks (Paper II). One test of these models is to look at the positional coincidence between powering sources and maser sites. The typical size of discs (<1000 au, or 10^{-3} pc) is much smaller than that of outflows (0.1 to a few pc). Thus a large offset between them would suggest an outflow origin for the maser emission. However, the proximity of the maser sites to the embedded source in all cases does not allow this conclusion to be made; within the errors the sites are no more than 3 arcsec apart, corresponding to a maximum of $\sim 10^4$ au for the three maser sources.

Another test of the two models is to look at the relative orientation between the H_2 emission and distribution of maser sites. There are sources where the methanol masers are distributed along a line, typically of order 1000 au in length (Norris 2000). Assuming an outflow comes out along the rotational axis of a circumstellar disc (e.g. Shu, Adams & Lizano 1987, and references therein), a perpendicular orientation of H_2 emission (where it traces an outflow) to methanol maser emission would favour the circumstellar disc hypothesis for the masers, and a parallel orientation would support the outflow origin. However, only in the case of IRAS 16076−5134 does the geometry appear clear.

(i) In G318.95–0.20, the maser sites show a linear distribution in a north–south direction (Norris et al. 1993; Paper II). With no significant velocity gradient or obvious outflow morphology observed in H_2 emission, we cannot conclude that there is an outflow. We thus have to rely on the absence of UV radiation to infer that the H_2 emission is likely shock-excited.

(ii) The velocity gradient in the H_2 emission towards IRAS 15278–5620 is indicative of outflow activity. This IRAS source has two maser sites located within 5 arcsec of each other, and two embedded NIR sources are found associated with them. The offset of these two maser sites exactly matches that of two stars at 3.3 μm (Paper III), but it is not clear which one is powering the outflow. Paper II does not find a linear distribution of the maser spots for either site, and Norris et al. (1993) also report a complex maser site. Thus no comparison with the direction of the outflow can be made.

(iii) For IRAS 16076–5134, an east–west outflow pattern is delineated by the H_2 emission, while Norris et al. (1993) report a north–south linear orientation of the maser site. This provides evidence for the methanol maser emission arising from a circumstellar disc, rather than being associated with an outflow.

4.3 Evolutionary sequence for massive star formation

4.3.1 Methanol maser emission and UC H II regions

Walsh et al. (Papers I, II) proposed an evolutionary sequence for high-mass star formation where methanol maser emission turns on during the protostellar phase (in which a molecular cloud core is still collapsing before hydrogen has started burning), then a star creates an UC H II region. Maser emission is turned off at an early stage of the UC H II region (Paper II). This was disputed by Phillips et al. (1998), who assumed the lack of detected radio continuum emission associated with methanol maser sites was because the maser sites are associated with lower mass non-ionizing stars (later than about B3).

We favour Walsh et al.'s evolutionary hypothesis, and present the following points to support the case for the pre-UC H II origin of methanol maser sites.

(i) Indirect support can be found in the observational evidence that methanol is more abundant towards high mass protostars than towards low-mass and field stars (Dartois et al. 1999).

(ii) In Paper I, the distribution of methanol maser sites around the Galactic plane was found to be consistent with a Galactic scaleheight of $0.^\circ4 \pm 0.^\circ1$, corresponding to a FWHM of $0.^\circ5 \pm 0.^\circ1$. Kurtz, Churchwell & Wood (1994) showed that the distribution of UC H II regions about the Galactic plane is $0.^\circ5 \leq |b_{\mathrm{FWHM}}| \leq 0.^\circ8$. Thus, the distribution of methanol maser sources is at least as tight as that of the UC H II regions, and possibly even tighter. This implies, as the most luminous sources

have the tightest distribution about the Galactic plane, that the majority of methanol maser sites come from the most luminous (ionizing) stars in the Galaxy. This is inconsistent with Phillips et al.'s assumption that maser emission is excited by non-ionizing stars. As 75 per cent of the maser sites are not associated with UC H II regions, yet their distribution about the Galactic plane is at least as tight, it seems unlikely they are all associated with non-ionizing stars.

(iii) In Paper II, it was found that those UC H II regions associated with methanol maser sites are smaller, and thus presumably younger, than the general population of UC H II regions imaged in that survey. This suggests the maser emission is seen at the earliest stages of formation of an UC H II region and disappears as the UC H II region evolves and expands.

(iv) One methanol maser source (IRAS 15541–5349) reported in Paper III was found to have an associated embedded source with a bolometric luminosity (inferred from the IR luminosity) commensurate with that of an ionizing star. However, no radio continuum emission was detected, i.e. when such a (ionizing) star is present, a UCH II region has not yet formed. This is supporting evidence for the pre-UC H II origin of methanol maser emission, i.e. when this type of (ionizing) star is present, an UC H II region has not yet formed.

(v) Cesaroni et al. (1994) reported the detection of hot ammonia cores towards three massive star-forming regions (G9.62+0.19, G29.96−0.02, and G31.41+0.31), which were interpreted as a pre-main-sequence stage of massive star formation. In each case, there is methanol maser emission associated with the ammonia clump (Paper II). Both the maser sites and ammonia clumps are offset from an UC H II region. This again supports the pre-UC H II origin of methanol maser emission.

(v) The results of this paper show methanol maser emission is associated with the powering sources of outflows, traced by shocked H_2 emission. Such outflows are thought to occur only during an early stage of star formation.

These points demonstrate that the majority of methanol maser sites are indeed associated with massive (possibly ionizing) stars before the UC H II region can be seen. As methanol maser emission is easily detectable throughout the Galaxy, and as it signposts such an early stage in massive star formation, it is potentially the most useful tool currently available for identifying massive protostellar sources. It is still possible, however, that a number of maser sites arise from lower mass (non-ionizing) stars because there is no a priori reason why the stellar mass cut-off limit for maser emission should be the same as that of ionizing radiation. In such a case, the number of these non-ionizing stars, inferred from the tight distribution of methanol maser sites around the Galactic plane, must be small compared with the number of maser sites associated with pre-UC H II ionizing stars.

4.3.2 Methanol maser emission and HMCs

The existence of compact, dense hot molecular cores (HMCs) has been well established by various observations (eg. Plume, Jaffe & Evans 1992). HMCs are believed to be sites of massive star formation (Kurtz et al. 2000), and may represent an earlier stage in the star formation process than UC H II regions (Codella, Testi & Cesaroni 1997). Hot core chemistry has shown that molecules, such as ammonia, water and methanol on the icy grain mantles, evaporate at the temperature ($\geq$100 K) of HMCs over a time-scale of 10^4 to 10^5 yr (see review by van Dishoeck & Blake 1998). Now with HMCs being the sites of massive star formation and with methanol maser emission signposting an earlier stage of massive star formation, we hypothesize that the methanol maser emission comes from HMCs.

An interesting question to address is that of when methanol maser emission commences and terminates? When a massive stellar core is formed from the infall of gaseous material, it reaches the main sequence before it stops accreting. This is followed by

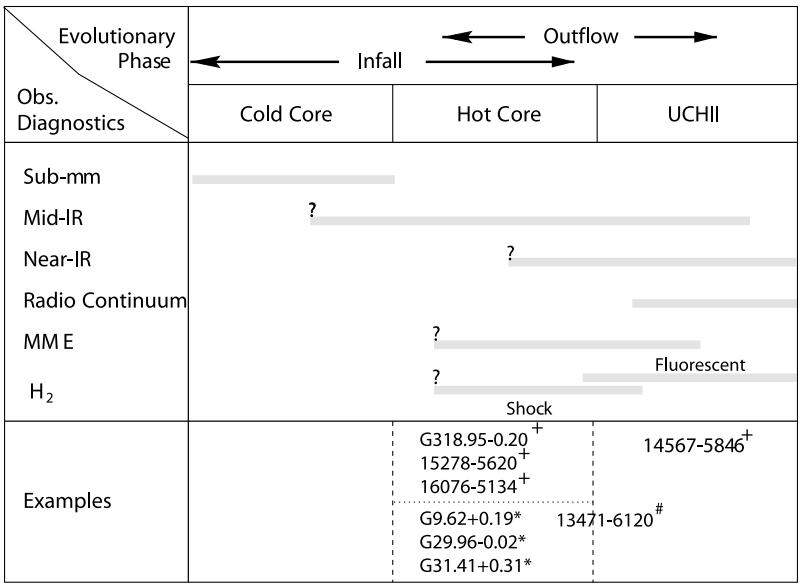

Figure 6. Our proposed evolutionary sequence leading to massive star formation. The phases in the sequence are listed horizontally and the observational signatures for it vertically. Shaded areas indicate when an observational diagnostic may be observable during the evolutionary sequence. The question mark is used when the beginning of the phase is uncertain, and MME stands for methanol maser emission. The sources marked with '+' are from this work, and those with '*' are hot NH_3 cores reported by Cesaroni et al. (1994). In IRAS 13471−6120 (marked with a '#'), an embedded NIR source is found coincident with both maser emission and an UC H II region (Paper III). If the pre-UC H II origin for methanol maser emission is correct, this source is in a transitional phase where the UC H II region is too young to have turned off the methanol maser emission.

formation of an UC H II region, with copious UV photons produced by the star (Garay & Lizano 1999). We propose that the formation of massive stars begins in HMCs where (1) heat from contraction releases methanol from the grain surface into the gas phase; (2) the gas is compressed, by outflows and/or in circumstellar discs, to create a sufficient column for masing – this stage is signposted by methanol maser emission and shocked H_2 line emission; (3) As the UC H II region expands, it turns off methanol maser emission and forms a PDR envelope where H_2 is excited by UV fluorescence.

This scenario is summarized in Fig. 6, where we attempted to fit observational diagnostics of massive star formation into the evolutionary sequence they represent. Based on this, we suggest that UC H II region IRAS 14567−5864 is at a later stage of massive star formation than other methanol maser sources observed. Hot ammonia cores from Cesaroni et al. (1994) are also presented in their corresponding evolutionary stage in Fig. 6.

There are questions still unanswered. When does methanol maser emission commence and terminate? Does it commence during the infall/accretion phase or later in the outflow phase? How long does methanol maser emission survive after an UC H II region has formed? One test is to look for cold molecular cores in the submillimetre, and determine any association with methanol maser emission. Such an association would be definite proof of the methanol maser emission being the signpost of an early stage of massive star formation. In addition, spectral energy distributions of the powering sources would help determine their spectral type, enabling us to discern between the pre-UC H II origin and non-ionizing star origin for methanol maser emission.

5 SUMMARY

We report the discovery of H_2 1–0 S(1) 2.12-μm line emission associated with one UC H II region and three methanol maser sites. The H_2 emission is excited by UV fluorescence in the case of the UC H II region IRAS 14567–5846, and traces the outer boundary of the UC H II region. The other three regions (G318.95–0.20, IRAS 15278–5620 and IRAS 16076–5134) all show convincing evidence for shock-excited H_2 emission: G318.95–0.20 shows strong H_2 emission, but no outflow can be discerned in either the morphology or the velocity structure of H_2 emission. IRAS 15278–5620 shows a fan-shaped, blueshifted outflow, stemming from two sites of maser emission. It is not clear which source is powering the outflow. Extended H_2 emission is also found to the north of the maser sites, but we suspect that this arises from a separate source.

In the case of IRAS 16076–5134, we report the detection of an outflow shown by highly blueshifted H_2 emission offset from an extremely deeply embedded object, the maser emission of which falls along a line perpendicular to that of the outflow. We interpret this as evidence of a circumstellar disc origin for the maser emission. Along with the detection of outflows traced by H_2 emission in this paper, we summarize evidence available to support the hypothesis that methanol maser emission appears before UC H II regions. Then we propose further that the methanol gas, released from grains in HMCs, is compressed to emit maser emission either by outflows or in circumstellar discs of protostars. H_2 is excited by shocks during the outflow phase, and by UV photons later during the UC H II region phase. An evolutionary sequence leading to massive star formation is proposed.

ACKNOWLEDGMENTS

We thank the AAT staff for their support during the observations, and Drs Lori Allen and Stuart Ryder for their valuable help during the UNSWIRF reduction.

REFERENCES

Allen D. A. et al., 1993, Proc. Astron. Soc. Aust., 10, 298
Burton M. G., 1992, Aust. J. Phys., 45, 463
Caswell J., Vaile R., Ellingsen S., Whiteoak J., Norris R., 1995, MNRAS, 272, 96
Cesaroni R., Churchwell E., Hofner P., Walmsley M., Kurtz S., 1994, A&A, 288, 903
Codella C., Testi L., Cesaroni R., 1997, A&A, 325, 282
Dartois E., Schutte W., Geballe T., Demyk K., Ehrenfreund P., d'Hendecourt L., 1999, A&A, 342, L32
Ellingsen S., Norris R., McCulloch P., 1996, MNRAS, 279, 101
Garay G., Lizano S., 1999, PASP, 111, 1049
Hollenbach D., McKee C. F., 1989, ApJ, 342, 306
Kawamura J. H., Masson C. R., 1998, ApJ, 509, 270
Kurtz S., Churchwell E., Wood D., 1994, ApJS, 91, 659
Kurtz S., Cesaroni R., Churchwell E., Hofner P., Walmsley M., 2000, in Mannings V., Boss A., Russell S., eds, Protostars and Planets IV. Univ. Arizona Press, Tucson, p. 299
Menten K. M., 1991, ApJ, 380, 75
Menten K. M., 1996, in van Dishoeck E. F., ed, IAU Symp. 178, Molecules in astrophysics: probes and processes. Kluwer, Dordrecht, p. 163
Norris R. P., 2000, in Minh Y. C., van Dishoeck E. F., eds, IAU Symp. 197: Astrochemistry – From Molecular Clouds to Planetary Systems. Astron. Soc. Pac., San Francisco, p. 223
Norris R. P., Whiteoak J. B., Caswell J. L., Wieringa M. H., Gough R. G., 1993, ApJ, 412, 222
Norris R. P. et al., 1998, ApJ, 508, 275
Phillips C. J., Norris R. P., Ellingsen S. P., McCulloch P. M., 1998, MNRAS, 300, 1131
Plume R., Jaffe D. T., Evans N. J., II, 1992, ApJ, 78, 505
Ryder S. D., Sun Y.-S., Ashley M. C. B., Burton M. G., Allen L. E., Storey J. W. V., 1998, Proc. Astron. Soc. Aust., 15, 228
Shu F. H., Adams F. C., Lizano S., 1987, ARA&A, 25, 23
Slysh V., Val'tts I., Kalenskii S., Voronkov M., Palagi F., Tofani G., Catarzi M., 1999, A&A, 134, 115
van Dishoeck E. F., Blake G. A., 1998, ARA&A, 36, 317
Walsh A. J., Hyland A. R., Robinson G., Burton M. G., 1997, MNRAS, 291, 261 (Paper I)
Walsh A. J., Burton M. G., Hyland A. R., Robinson G., 1998, MNRAS, 301, 640 (Paper II)
Walsh A. J., Burton M. G., Hyland A. R., Robinson G., 1999, MNRAS, 309, 905 (Paper III)
Walsh A. J., Bertoldi F., Burton M. G., Nikola T., MNRAS, 2001, in press

This paper has been typeset from a TEX/LATEX file prepared by the author.